

Role of B-cells in Mycosis Fungoides

Pia Rude NIELSEN^{1,2}, Jens Ole ERIKSEN¹, Mia Dahl SØRENSEN³, Ulrike WEHKAMP⁴, Lise Maria LINDAHL⁵, Michael BZOREK¹, Lars IVERSEN⁵, Anders WOETMAN², Niels ØDUM², Thomas LITMAN² and Lise Mette Rahbek GJERDRUM^{1,6}

¹Department of Pathology, Zealand University Hospital, Roskilde, ²Leo Foundation Skin Immunology Research Center, Department of Immunology and Microbiology, University of Copenhagen, Copenhagen, ³Department of Pathology, Odense University Hospital, Odense, Denmark, ⁴Department of Dermatology, University Hospital, Schleswig-Holstein, Kiel, Germany, ⁵Department of Dermatology, Aarhus University Hospital, Aarhus and ⁶Institute for Clinical Medicine, University of Copenhagen, Copenhagen, Denmark

Mycosis fungoides is the most common type of cutaneous T-cell lymphoma. The inflammatory microenvironment in mycosis fungoides is complex. There is accumulating evidence that the neoplastic T-cells take control of the microenvironment and thereby promote their own expansion by suppressing cellular immunity. B-cells have proved to be upregulated in large-cell transformed mycosis fungoides, and could potentially play a role in disease progression. To investigate the presence of B-cells in mycosis fungoides compared with controls, this study analysed 85 formalin-fixed and paraffin-embedded mycosis fungoides biopsies. *MS4A1* gene expression was significantly upregulated in mycosis fungoides compared with controls ($p < 0.0001$) and further upregulated in disease progression, ($p = 0.001$). Digital quantification of PAX5⁺/CD20⁺ cells confirmed the increased presence of B-cells in mycosis fungoides compared with controls. No co-labelling of CD3/CD20 was observed in the neoplastic T-cells. This study found a significantly increased presence of B-cells in the tumour-associated microenvironment in mycosis fungoides. These findings could potentially lead to new treatment strategies for mycosis fungoides.

Key words: B-cells; cutaneous T-cell lymphoma; mycosis fungoides; tumour microenvironment.

Accepted Feb 23, 2021; Epub ahead of print Mar 9, 2021

Acta Derm Venereol 2021; 101: adv00413.

Corr: Pia Rude Nielsen, Department of Pathology, Zealand University Hospital, DK-4000 Roskilde, Denmark. E-mail: pirn@regionsjaelland.dk

Cutaneous T-cell lymphomas (CTCLs) are a heterogeneous group of non-Hodgkin lymphomas in the skin. The predominant subtype is mycosis fungoides (MF), comprising approximately 60% of all CTCLs (1). Other subtypes of CTCL include Sézary syndrome (SS), primary cutaneous CD30⁺ lymphoproliferative disorders, and some other rare variants according to the World Health Organization (WHO) classification of tumours of haematopoietic and lymphoid tissues (2) and the classification of cutaneous lymphomas by the WHO and European Organization for Research and Treatment of Cancer (EORTC) (1, 3).

Despite decades of research, the pathogenesis of MF is only partly understood. A number of possible pathogenic

SIGNIFICANCE

The inflammatory microenvironment in mycosis fungoides is complex, and little is known about the presence of B-cells in this disease. This retrospective study examined 85 biopsies from patients with all stages of mycosis fungoides. *MS4A1* gene expression was significantly upregulated in mycosis fungoides compared with controls, and further upregulated in disease progression. Digital quantification of double (PAX5/CD20)-stained slides confirmed the increased presence of B-cells in mycosis fungoides compared with controls. No aberrant CD20 expression was found in the neoplastic T cells. These findings could potentially promote new treatment strategies for mycosis fungoides.

factors, especially genetic and epigenetic events, have been explored in MF, including recurrent mutations and deletions (4–7). Deregulation of microRNAs (miRNAs) has been identified as an important epigenetic mechanism in a wide range of cancers, and several miRNAs have been associated with MF, where miR-155, miR-22 and miR-29b have been implicated in the pathogenesis of MF (8–11). In addition, environmental factors, such as bacterial infections, have been linked with disease progression, and antibiotic treatment of skin infections with *Staphylococcus aureus* has proven to clinically improve skin symptoms and inhibit the malignant T-cells in patients with MF (12–14).

Furthermore, the tumour-associated inflammatory microenvironment and changes herein have been outlined as a critical point in the transition from indolent to advanced disease stage, where the neoplastic T-cells are suspected to be involved in driving the inflammatory environment from anti-tumourigenic to pro-tumourigenic by the production of a wide variety of distinct chemokines and cytokines (15, 16). Moreover, the malignant T-cells have also been suspected to exploit innate immune cells, such as monocytes and dendritic cells, to proliferate and prolong their own survival. Interestingly, the malignant T-cells have been shown to keep the dendritic cells in an immature state by secretion of interleukin 10 (IL-10), thereby maintaining a tolerogenic immune microenvironment. In addition, IL-10-producing regulatory B-cells (Bregs) are significantly decreased in advanced-stage MF (AS-MF) compared with controls (17). B-cells, especially Bregs, have been shown to

play an important role in a range of inflammatory and autoimmune diseases (18), but studies concerning the presence of B-cells in patients with MF are sparse. A previous study from Shin et al. (19) reported several upregulated B-cell related genes in MF, and Krejsgaard et al. (20) showed ectopic expression of B-lymphoid kinase (Blk), primarily related to the epidermotropic T-cells. These findings could contribute to the diagnostic workup of early-stage MF (ES-MF). An abundant population of CD20-positive B-cells has also been described in some cohorts of transformed MF (T-MF) (21, 22).

In a previous gene expression study utilizing NanoString technology, we found that the *MS4A1* (CD20) gene was highly upregulated in ES-MF and AS-MF compared with controls (23). This prompted us to further characterize these findings and elucidate whether CD20 upregulation was due to increased presence of B-cells in MF, or to a combination of the increased number of B-cells and aberrant CD20 expression in the neoplastic T-cells.

MATERIALS AND METHODS

Patients and samples

This study analysed a total of 85 formalin-fixed and paraffin-embedded (FFPE) skin biopsies from 69 patients with either ES-MF (\leq IIA) or AS-MF ($>$ IIA). The majority of the samples ($n=58$) were collected from the archives at the Department of Pathology, Zealand University Hospital, Denmark, as previously described (24). In addition, 27 FFPE samples were provided from the Department of Dermatology, Aarhus University Hospital, Denmark and the Department of Dermatology, University Hospital, Schleswig-Holstein, Kiel, Germany (23). All slides for diagnostic workup were histologically re-evaluated, and clinical records were reviewed for establishing diagnosis and clinical stage according to the diagnostic criteria of MF (25). A control group included FFPE skin biopsies from patients with chronic, unspecified dermatitis (D) ($n=46$) and healthy skin from breast reduction surgery (HS) ($n=11$).

The study was approved by the Data Protection Agency (J.NR. REG-009-2017) and the local ethics committees (SJ-603, B249/16 and 1-10-72-91-13).

Gene expression analysis

Total RNA extraction was performed using Roche high pure RNA FFPE isolation kit (Roche Life Science, Mannheim, Germany) according to the manufacturer's guidelines. Gene expression analysis was performed using NanoString platform (NanoString Technologies, Seattle, WA, USA) with the nCounter Human Myeloid Innate Immunity Panel v2 (NanoString Technologies), complemented with an additional 30 genes of interest as described previously (23). Total RNA input for each sample extracted from FFPE tissues ranged from 50 to 100 ng, with an A260/280 absorbance ratio between 1.5 and 2.1. Direct hybridization of unique barcodes to target RNAs were analysed on the Prep Station and digital detection and counting of the hybridized probes were performed on the digital analyser. Normalization factors were calculated based on 40 housekeeping genes included in the myeloid innate immunity panel using nSolver™ software. All procedures were performed following the NanoString guidelines.

Data availability statement

Data related to this article are available in GEO (<https://www.ncbi.nlm.nih.gov/geo/query/acc.cgi?acc=GSE143382>) with accession number GSE143382.

Sequential double-immune-labelling technique

Double-immuno-labelling experiments were performed on 3- μ m-thick FFPE sections, using anti-human PAX5 clone DAK-Pax5 (Agilent/Dako, cat. no. M7307, Glostrup, Denmark) and CD20 clone L26 (Agilent/Dako, cat. no. M0755). All incubation steps were performed automatically on the Omnis (Agilent/Dako). Briefly, FFPE sections were exposed to deparaffinization, followed by antigen retrieval using EnVision™ FLEX Target Retrieval solution (3-in-1) pH 9 (Agilent/Dako, cat. no. GV800/821) at 97°C (24 min). In the first sequence, slides were incubated with PAX5 diluted 1:30 in Renoir Red (Biocare Medical, cat. no. PD904, Pacheco, CA, USA) for 30 min (32°C), and reactions were visualized with EnVision™ FLEX /HRP/DAB Detection Reagent (Dako, cat. no. GV800/GV821). After visualization with DAB, slides were incubated with CD20, diluted 1:500 in Envision Flex Antibody Diluent (Agilent/Dako, cat. no. K8006) for 30 min (32°C), reactions were detected with EnVision™ FLEX/HRP Reagent (Dako, cat. no. GV800/GV821) and visualized using Magenta Substrate chromogen system (Agilent/Dako, cat. no. GV925). All slides were counterstained with haematoxylin and mounted with Pertex.

Image analysis of PAX5⁺/CD20⁺ cells

All CD20/PAX5-stained FFPE samples were digitalized and evaluated using Visiopharm Integrated System (VIS) software module (Version 2018.9.4, Visiopharm, Hørsholm, Denmark). Epidermis and islets of dermis were defined as a region of interest and manually outlined, excluding areas containing staining-artefacts and areas of dermal non-nucleated cells. The images were analysed and quantified using an automatic cell classification-based algorithm developed by VIS. The first step was to identify all nuclei using the red colour band feature (RGB-R band). Subsequently, a 1.7- μ m perimeter was grown around all detected nuclei to identify the cell cytoplasm. The cytoplasm was separated into positive and negative cytoplasm based on the CD20 expression and using the haematoxylin-DAB colour band showing DAB structures (HDAB-DAB colour-band feature). Next, the algorithm was optimized using post-processing steps available in the VIS software, and the nuclei was divided into a positive or a negative cell population based on nuclear expression of PAX5 and using Liquid Permanent Red and DAB colour band showing DAB structures (Fast Red DAB-DAB colour-band feature). Finally, the nuclei were subdivided further into populations, based on whether they were surrounded by CD20⁺-cytoplasm, overall generating 4 outcomes: (1) PAX5⁺/CD20⁺, (2) PAX5⁺/CD20⁻, (3) CD20⁺/PAX5⁻, (4) PAX5⁻/CD20⁻. Areas of each cell population, double-positive cell population as well as the total nuclei area were defined as output variables, and area fractions for each population were quantified using the total nuclei area as the denominator.

Double-immunofluorescence staining with CD3 and CD20

Double-immunofluorescence (dIF) studies (simultaneous technique) were performed on representative cases (5 ES-MF and 2 AS-MF) to investigate whether the neoplastic T-cells and the sub-population PAX5⁻/CD20⁺ cells were malignant T-cells displaying an aberrant CD20 expression. The dIF staining was performed as described in detail elsewhere (26). In brief, after deparaffinization and antigen retrieval, as described above, the slides were incubated for 30 min (32°C) with a mixture of anti-human CD3

clone EP41 (Cell Marque, cat. no. AC-0004, Rocklin, CA, USA) and anti-human CD20 clone L26 (Agilent/Dako, cat. no. M0755) diluted in Renoir Red (Biocare, cat. no. PD904) 1:20 and 1:250, respectively. Slides were incubated with a mix of goat anti-rabbit conjugated with Alexa Fluor 594 (Fisher Scientific, cat. no. 11012, Roskilde, Denmark) and goat anti-mouse conjugated with Alexa Fluor 488 (Fisher Scientific, cat. no. 11001), both diluted 1:200 in Envision Flex Antibody Diluent (Agilent/Dako, cat. no. K8006), for 30 min (32°C). After washing, the slides were air-dried and mounted with Vectashield with DAPI (Vector Labs, cat. no. H1200, Burlingame, CA, USA). Slides were evaluated with a Nikon Eclipse 80 fluorescence microscope with standard sets of filters for each fluorochrome.

Statistical analysis

Gene expression data was analysed by 2-way analysis of variance (ANOVA) with Tukey's *post hoc* test (which corrects for multiple testing), and cohort eliminated as a factor. Digital analysis of the double-immunohistochemically stained slides was performed in GraphPad Prism (version 8.1.1, GraphPad Software, Inc., San Diego, CA, USA) by the non-parametric Kruskal–Wallis test and significance was adjusted for multiple testing by estimating false discovery rate (FDR) by the 2-stage step-up method of Benjamini et al. (27). A significance level of 5% ($\alpha=0.05$) was considered statistically significant. For visualization on a log-scale, 0 (zero) values were floored to 0.001.

RESULTS

Patient and sample characteristics

The mean age at time of MF diagnosis was 63.8 years (range 18–84 years) and 40 males and 29 females (58%/42%) were included. Information on clinical stage and treatment at the time of biopsy is listed in **Table I**. The mean age of the dermatitis control group was 58.4

years (range 23–88 years) and the male to female ratios were almost equal (1:1.1). The lymphocytic infiltrate ranged from discrete to moderate superficial dermal and perivascular infiltration with varying degrees of exocytosis. The mean age of the healthy skin control group was 71.5 years (range 46–83 years).

MS4A1 (CD20) gene expression analysis in the study cohort and validation cohort

MS4A1 gene (CD20) expression was significantly higher in both ES-MF and AS-MF compared with controls (**Fig. 1**). Median *MS4A1* gene expression (normalized mRNA counts) was significantly elevated in ES-MF 12.5 [8.2;29.6] compared with D 2.6 [1.7;4.1], $p<0.0001$ and to HS 1.0 [1.0;2.8], $p<0.0001$. Likewise, *MS4A1* gene expression was significantly higher in AS-MF 87.2 [26.8;272.4] compared with D 2.6 [1.7;4.1], $p<0.0001$ and HS 1.0 [1.0;2.8], $p<0.0001$. *MS4A1* gene expression was significantly upregulated in AS-MF compared with ES-MF (fold-change 5.2, $p=0.001$). There was no statistically significant difference between the medians of the D and HS ($p=0.1$) samples.

Digital analysis of PAX⁺/CD20⁺ immunostained cells

To evaluate protein expression of PAX5⁺/CD20⁺ cells, double-immunohistochemical staining was performed on 58 MF (both early- and advanced-stage MF), 29 D and 11 HS FFPE samples, referring to the cohort collected from the Department of Pathology, Zealand University Hospital. Furthermore, this study aimed to investigate whether overall CD20 expression was related to B-cells, or whether some of these cells were neoplastic T-cells

Table I. Clinical characteristics at time of biopsy

Characteristics	Cohort n = 85 n (%)
Clinical stage	
IA	43 (50.6)
IB	22 (25.9)
IIA	1 (1.2)
IIB	10 (11.8)
III	3 (3.5)
IVA	1 (1.2)
IVB	0 (0)
No data available	5 (5.9)
T-stage	
T1	45 (52.9)
T2	21 (24.7)
T3	10 (11.8)
T4	4 (4.7)
No data available	5 (8.6)
Treatment ^a	
No treatment	13 (15.3)
Topical steroids	31 (36.5)
Other ^b	11 (12.9)
Two or more treatments ^c	7 (8.2)
No data available	23 (27.1)

^aTreatment at time of biopsy. ^bOther treatment strategies includes ultraviolet B (UVB), psoralen plus ultraviolet A (PUVA), nitrogen mustard, methotrexate, neotigason and extracorporeal photopheresis. ^cTopical steroid in combination with other treatment modalities (e.g. UVB, PUVA and/or systemic treatment).

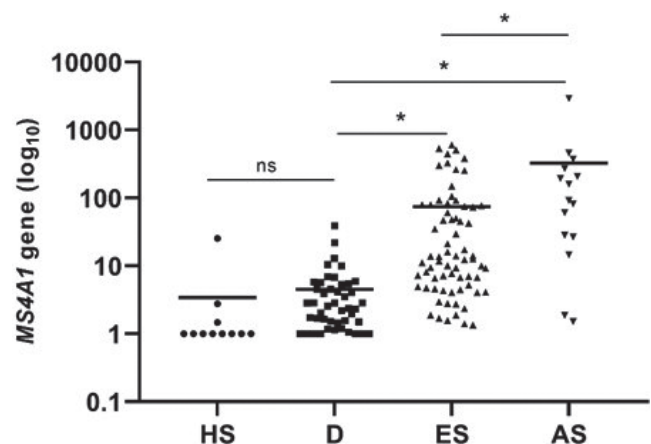


Fig. 1. *MS4A1*-gene (CD20) expression in patients with mycosis fungoides (MF) compared with controls. Significant upregulation of *MS4A1* in early-stage (ES) MF and advanced-stage (AS) MF is observed compared with controls. Also, significant upregulation of *MS4A1* gene expression in AS-MF compared with ES-MF (fold-change = 5.2, $p=0.002$) was seen. There was no significant difference in *MS4A1* gene expression between controls (dermatitis (D) and healthy skin (HS) ($p=0.541$)). Horizontal lines represent median, ns: not significant, *indicate $p<0.05$ by 2-way analysis of variance (ANOVA) and Tukey's *post hoc* test.

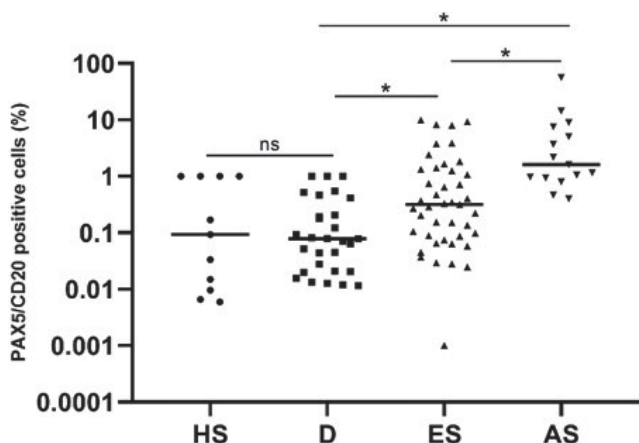


Fig. 2. Digital quantification of the double-immunohistochemical stained slides with PAX5 and CD20 in patients with mycosis fungoides (MF). Scatter plot of the digital image analysis of PAX5⁺/CD20⁺ cells, shows the fraction of double-positive cells of all nucleated cells as a percentage. Presence of B-cells is significantly increased in early-stage (ES) MF and advanced-stage (AS) MF compared with the controls of dermatitis (D) and healthy skin (HS). The number of B-cells was significantly upregulated in AS-MF compared with ES-MF ($p < 0.005$). No significant differences were observed between D and HS ($p = 0.113$). Horizontal lines represent mean, ns: not significant, *indicates $p < 0.05$ by Kruskal–Wallis test.

with an aberrant expression of CD20. The PAX5⁺/CD20⁺ cells were digitally quantified, and the results are visualized in **Fig. 2**. The median fraction of PAX5⁺/CD20⁺ cells of all nucleated cells, in percentage, was 0.32 [0.14;0.71] in ES-MF, 1.61 [0.94;7.59] in AS-MF, 0.08 [0.03;0.19] in D, and 0.09 [0.001;1] in HS. The fraction of the digitally analysed PAX5⁺/CD20⁺ cells was significantly increased between ES-MF and AS-MF ($p = 0.005$) and the fraction of B-cells in both ES-MF and AS-MF was significantly higher compared with D ($p = 0.0002$, $p < 0.0001$, respectively) and HS ($p < 0.0001$, $p < 0.0001$, respectively). There was no significant difference in the presence of PAX5⁺/CD20⁺ cells between D and HS ($p = 0.11$) (Fig. 2).

The distribution pattern of PAX5⁺/CD20⁺ B-cells was diverse, ranging from diffusely scattered single cells to a denser band-like infiltrate in the dermal compartment. Some biopsies presented with both perifollicular and perivascular infiltrates of B-cells. The morphology of the PAX5⁺/CD20⁺ cells in the majority of the samples was small-to-medium-sized B-lymphocytes with no atypical appearance, suggesting their reactive nature. One patient with AS-MF (stage IIB) had a dense dermal infiltrate of >50% large, CD20⁺ centroblast-like B-cells with reactive germinal centres. The B-cell immunophenotype in this patient was positive for CD20, PAX5, CD23, BCL6, and the proliferation marker Ki67 was, as expected, higher in the germinal centres compared with the rest of the biopsy. Immunoglobulin (Ig) heavy chain clonality was negative, and there was no kappa/lambda light chain restriction. The neoplastic T-lymphocytes were positive for CD3 and CD4, but negative for CD8. The patient had clonally rearranged T-cell receptor genes in the skin. No large cell transformation (LCT) of the neoplastic

T-cells was observed, but the patient later transformed to large-cell MF and, at that time, there was still a significant presence of B-cells in the dermal infiltrate. **Fig. 3** illustrates PAX5/CD20 immunohistochemically stained slides in representative patients with ES-MF, AS-MF, dermatitis and healthy skin.

Double-immunofluorescence labelling with CD3 and CD20

In a few cases there was a minor population of PAX5⁻/CD20⁺ cells. Double CD3/CD20 immunofluorescence staining could not verify an aberrant CD20 expression in the neoplastic T-cells in these cases (**Fig. 4**).

Correlation between MS4A1 (CD20) and IL10 gene expression

This study did not attempt to identify different subtypes of CD20-positive cells, but a correlation analysis between CD20 and IL10 gene expression levels found no significant correlation between CD20 and IL10 gene expression in the subgroups of MF and dermatitis, either in patients with early-stage MF who progressed to a higher disease stage or in those patients who did not progress (data not shown).

DISCUSSION

This study analysed the presence of B-cells in patients with ES-MF and AS-MF compared with controls. In accordance with previously published papers, a significant upregulation of infiltrating B-cells was found in MF compared with controls (21, 28, 29). However, contrary to these findings, Iliadis et al. (30) reported absent or lower numbers of B-cells in the inflammatory micro-environment in various stages of MF. In the current study the morphology of PAX5⁺/CD20⁺ B-cells displayed, in most cases, small- to-medium-sized lymphocytes with no cytological atypia. The study cohort displayed no aberrant CD20 protein expression in the neoplastic T-cells, which has been reported previously (21, 31). An abundant proportion of CD20⁺ lymphoid cells in MF has previously been associated with poorer prognosis in T-MF (31), and the presence of <10% or >50% of tumour-infiltrating B-cells in patients with T-MF has been reported to have a negative prognostic impact compared with those with 10–49% tumour-infiltrating B-cells (21). However, this study consisted of relatively few patients; hence no firm conclusions can be drawn from the results, and the prognostic impact of the tumour-infiltrating B-cells in T-MF still needs to be further elucidated. The current study could not confirm the prognostic impact of tumour-infiltrating B-cells in early-stage disease, as no significant differences were found in CD20 expression between patients who progressed and those who did not

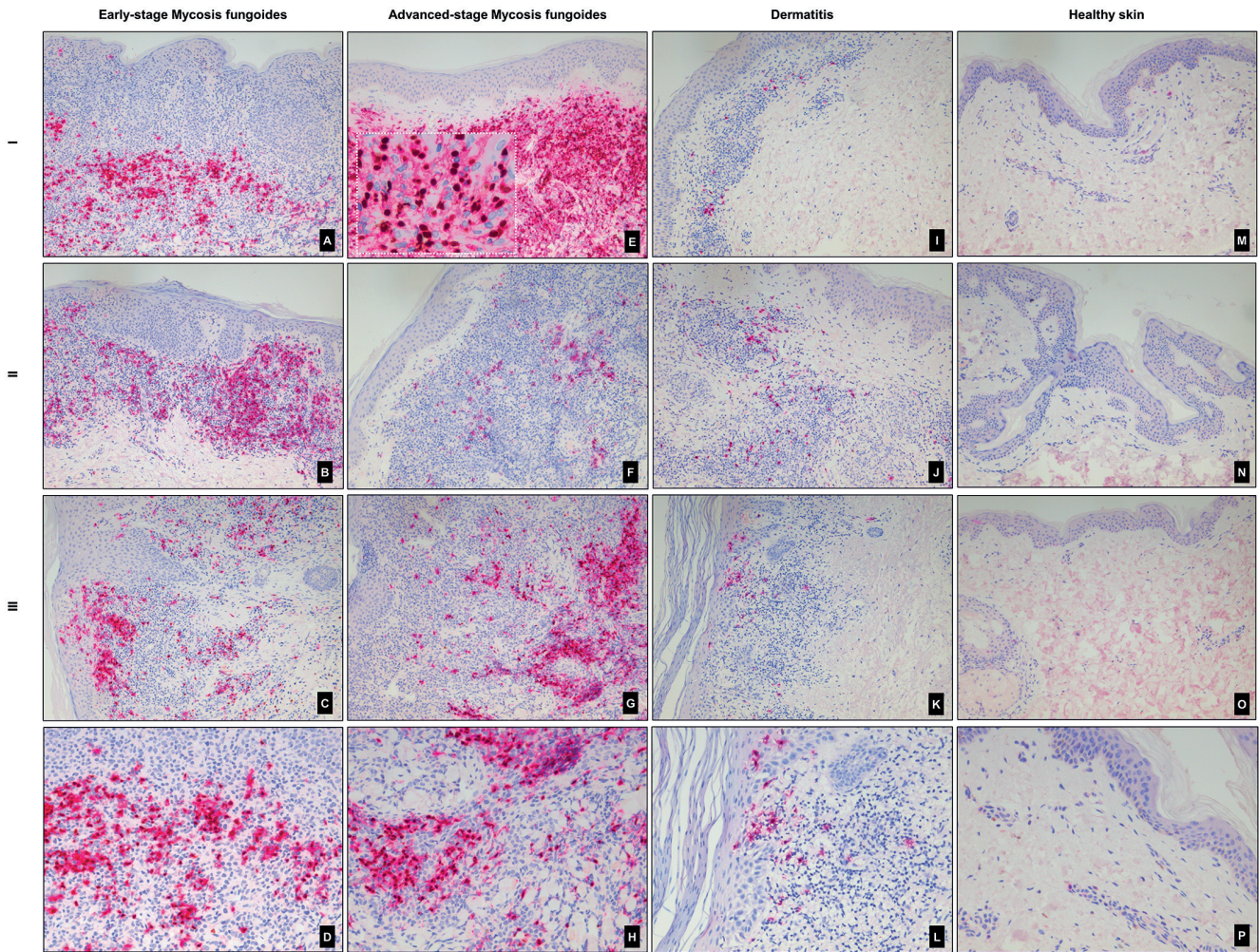


Fig. 3. Double-immunohistochemical staining with PAX5 (nucleus, brown) and CD20 (cytoplasm, magenta) in early-stage (ES) mycosis fungoides (MF), advanced-stage (AS) MF, dermatitis (D) and healthy skin (HS). Presence of double-immunostained small-to-medium-sized B-cells in 3 different patients with (A–C) ES-MF, (E–G) AS-MF, (I–K) D and (M–O) HS. (E) PAX5⁺/CD20⁺ large, atypical, centroblast-like B-cells in a patient with AS (non-transformed MF). (A–C, E–G, I–K) Original magnification ×100, (E) white dotted line higher power field (×600) of the double-immunostained B-cells. Higher power field (×200) of patients (D) A, (H) G, (L) K, and (P) M.

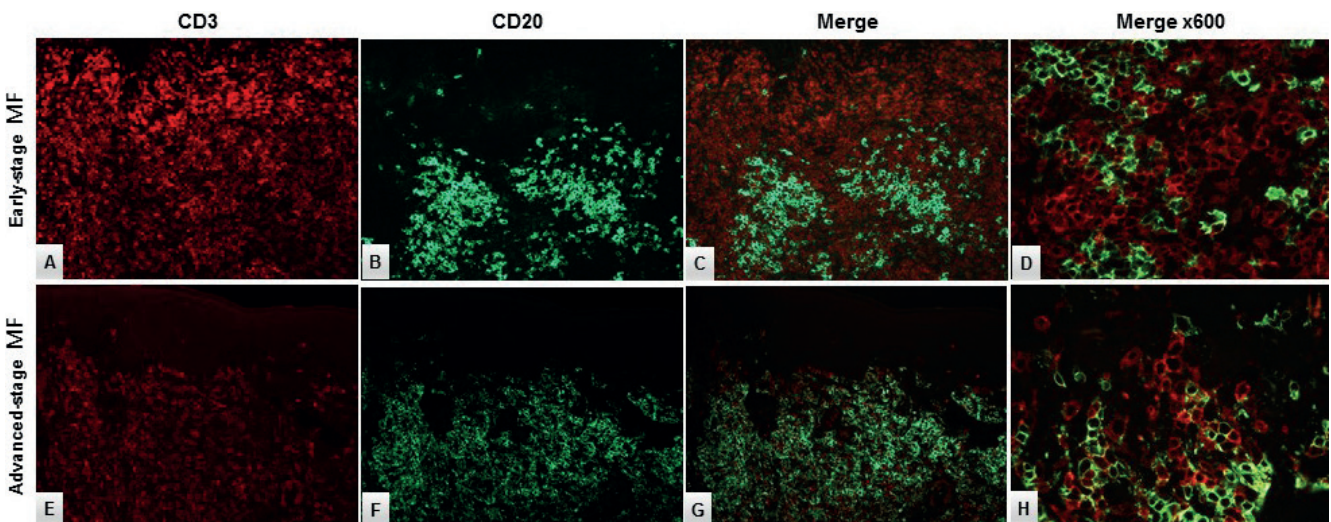


Fig. 4. Double-immunofluorescence staining with CD3 (red) and CD20 (green) in (A–D) early-stage (ES) mycosis fungoides (MF) and (E–H) advanced-stage (AS) MF. The neoplastic T-cells did not display aberrant CD20 expression (expected yellow reaction product) in (D) ES-MF or (H) AS-MF, respectively. Original magnification ×200 in A–C, E–G and ×600 in D, H.

(data not shown). The prominent B-cell population in some of the patients in the current cohort masked, to some extent, the true nature of the neoplastic T-cell infiltrate, thereby contributing to a delayed diagnosis.

The functional role of tumour-associated B-cells in the microenvironment of MF has not been fully clarified, but it seems that in various human solid tumours (e.g. lung, breast and ovarian cancer) the presence of B-cells improved tumour control and served as a positive prognostic factor (33, 34). On the other hand, absence of B-cells has been correlated with an improved tumour control in a murine breast cancer model (35). In addition, a subpopulation of IL-10-secreting Bregs has been identified as a negative inflammatory regulator that can facilitate breast cancer metastasis by initiating anti-tumour response (36). Furthermore, in several gastrointestinal cancers (colon, oesophagus and gastric cancer) upregulation of IL-10 secreting Bregs has been described as a poor prognostic factor, whereas, in advanced MF, the IL-10-secreting Bregs were decreased, and this could have an impact on the progression in MF (17). The current study did not find any correlation between the *CD20* and *IL10* gene expression levels, suggesting that the presence of the *CD20*⁺ cells was not related to IL-10-secreting Bregs.

Interestingly, a study from Theurich et al. (29) showed remarkable clinical regression and sustained complete remission of a nuchal MF tumour after local injection with the anti-*CD20* antibody rituximab. Moreover, flow-cytometric and histological analysis showed depletion of B-cells and *CD4*⁺ lymphoma cells and in addition, *FoxP3*⁺ regulatory T-cells were reduced and tumour-infiltrating *CD8*⁺ cytotoxic T-cells were increased after treatment with rituximab (29). Likewise, a study from Ghosn et al. reported a sustained improvement of MF in a patient who had concomitant Kimura disease treated with rituximab (37).

In conclusion, this study found a significant increase in B-cells in the tumour-associated microenvironment in patients with MF compared with controls. Furthermore, the number of B-cells increased significantly with disease progression; however, this study could not confirm the potential poor prognostic effect of the lymphoma-infiltrating B-cells in early-stage disease between patients who progressed and those who did not. These data prompt further questions: how do the infiltrating B-cells impact MF biology, and can we re-establish the immunological tumour control by targeting these cells therapeutically? A recent study implicates different roles for B-cells in atopic dermatitis (AD) and psoriasis (38). Here, AD revealed a higher incidence of *CD27*⁺ memory B-cells, plasmablast and *IgE*⁺ memory subsets. In contrast, psoriasis revealed B-cell subsets resembling those of healthy skin. In line with this, rituximab treatment of patients with AD led to disease improvement, abolished B-cell counts, decreased T-cell activation and IL-13

production in peripheral blood, together with reduction in *CD20*⁺, *CD4*⁺, *CD8*⁺ and *CD1a*⁺ cells in skin biopsies, and decreased mRNA expression of IL-13 and IL-5 (39). In contrast, anti-*CD20* therapy did not improve B-cell depletion in psoriasis (40) and, furthermore, treatment with rituximab could, in some patients, induce psoriasis lesions (41). This indicates opposite functional roles for B-cells in various T-cell mediated benign diseases. We hypothesize, that B-cells are implicated in the pathogenesis of MF, and hereby open a window for further studies elucidating the nature and functional role of various B-cell subsets in MF, which could potentially promote new treatment strategies in CTCL.

ACKNOWLEDGEMENTS

The technical assistance provided by the immunohistochemical and molecular team at the Department of Pathology, Næstved, Denmark is greatly appreciated.

This work was supported by the Danish Cancer Research Foundation (Dansk Kræftforskningsfond), Region Zealand Health and Research Foundation, the Region of Zealand and Southern Denmark Research Foundation, Aage Bang Foundation, LINAK A/S Nordborg, the Harboe Foundation, the carpenter Jørgen Holm and wife Elisa F. Hansen Memorial Foundation, the Medical Research Association Foundation and the A.P. Moeller Foundation.

LMRG has received funding from NanoString Technologies. T.L. is employed both by Copenhagen University and by LEO Pharma A/S. The remaining authors have no conflicts of interest to declare.

REFERENCES

1. Willemze R, Cerroni L, Kempf W, Berti E, Facchetti F, Swerdlow SH, et al. The 2018 update of the WHO-EORTC classification for primary cutaneous lymphomas. *Blood* 2019; 18: 1703–1714.
2. Swerdlow SH, Campo E, Pileri SA, Lee Harris N, Stein H, Siebert R, et al. The 2016 revision of the World Health Organization classification of lymphoid neoplasms. *Blood* 2016; 127: 2375–2390.
3. Willemze R, Jaffe ES, Burg G, Cerroni L, Berti E, Swerdlow SH, et al. WHO-EORTC classification for cutaneous lymphomas. *Blood* 2005; 105: 3768–3785.
4. McGirt LY, Jia P, Baerenwald DA, Duszynski RJ, Dahlman KB, Zic JA, et al. Whole-genome sequencing reveals oncogenic mutations in mycosis fungoides. *Blood* 2015; 23: 508–519.
5. Choi J, Goh G, Walradt T, Hong BS, Bunick CG, Chen K, et al. Genomic landscape of cutaneous T cell lymphoma. *Nat Genet* 2015; 47: 1011–1019.
6. Ungewickell A, Bhaduri A, Rios E, Reuter J, Lee CS, Mah A, et al. Genomic analysis of mycosis fungoides and Sézary syndrome identifies recurrent alterations in *TNFR2*. *Nat Genet* 2015; 47: 1056–1060.
7. Da Silva Almeida AC, Abate F, Khiabanian H, Martinez-Escala E, Guitart J, Tensen CP, et al. The mutational landscape of cutaneous T cell lymphoma and Sézary syndrome. *Nat Genet* 2015; 47: 1465–1470.
8. Ralfkiaer U, Hagedorn PH, Bangsgaard N, Løvendorf MB, Ahler CB, Svensson L, et al. Diagnostic microRNA profiling in cutaneous T-cell lymphoma (CTCL). *Blood* 2011; 118: 5891–5900.
9. Ralfkiaer U, Lindal L, Litman T, Gjerdrum LM, Ahler CB, Gniadecki R, et al. MicroRNA expression in early mycosis fungoides is distinctly different from atopic dermatitis and advanced cutaneous T-cell lymphoma. *Anticancer Res* 2014;

- 34: 7207–7217.
10. Sibbesen NA, Kopp KL, Litvinov I V., Jønson L, Willerslev-Olsen A, Fredholm S, et al. Jak3, STAT3, and STAT5 inhibit expression of miR-22, a novel tumor suppressor microRNA, in cutaneous T-cell lymphoma. *Oncotarget* 2015; 6: 20555–20569.
 11. Moyal L, Yehezkel S, Gorovitz B, Keren A, Gilhar A, Lubin I, et al. Oncogenic role of microRNA-155 in mycosis fungoides: an in vitro and xenograft mouse model study. *Br J Dermatol* 2017; 177: 791–800.
 12. Talpur R, Bassett R, Duvic M. Prevalence and treatment of *Staphylococcus aureus* colonization in patients with mycosis fungoides and Sézary syndrome. *Br J Dermatol* 2008; 159: 105–112.
 13. Lindahl LM, Willerslev-Olsen A, Gjerdrum LMR, Nielsen PR, Blümel E, Rittig AH, et al. Antibiotics inhibit tumor and disease activity in cutaneous T cell lymphoma. *Blood* 2019; 134: 1072–1083.
 14. Willerslev-Olsen A, Krejsgaard T, Lindahl LM, Bonefeld CM, Wasik MA, Koralov SB, et al. Bacterial toxins fuel disease progression in cutaneous T-cell lymphoma. *Toxins* 2013; 5: 1402–1421.
 15. Krejsgaard T, Lindahl LM, Mongan NP, Wasik MA, Litvinov I V., Iversen L, et al. Malignant inflammation in cutaneous T-cell lymphoma – hostile takeover. *Semin Immunopathol* 2016; 39: 269–282.
 16. Miyagaki T, Sugaya M. Immunological milieu in mycosis fungoides and Sézary syndrome. *J Dermatol* 2014; 41: 11–18.
 17. Akatsuka T, Miyagaki T, Nakajima R, Kamijo H, Oka T, Takahashi N, et al. Decreased IL-10-producing regulatory B cells in patients with advanced mycosis fungoides. *Eur J Dermatology* 2018; 28: 314–319.
 18. Miyagaki T, Fujimoto M, Sato S. Regulatory B cells in human inflammatory and autoimmune diseases: from mouse models to clinical research. *Int Immunol* 2015; 27: 495–504.
 19. Shin J, Monti S, Aires DJ, Duvic M, Golub T, Jones DA, et al. Lesional gene expression profiling in cutaneous T-cell lymphoma reveals natural clusters associated with disease outcome. *Blood* 2007; 110: 3015–3027.
 20. Krejsgaard T, Vetter-Kauczok CS, Woetmann A, Kneitz H, Eriksen KW, Lovato P, et al. Ectopic expression of B-lymphoid kinase in cutaneous T-cell lymphoma. *Blood* 2009; 113: 5896–5904.
 21. Jullié ML, Carlotti M, Vivot A, Beylot-Barry M, Ortonne N, Frouin E, et al. CD20 antigen may be expressed by reactive or lymphomatous cells of transformed mycosis fungoides: Diagnostic and prognostic impact. *Am J Surg Pathol* 2013; 37: 1845–1854.
 22. Vergier B, de Muret A, Beylot-Barry M, Vaillant L, Ekouevi D, Chene G, et al. Transformation of mycosis fungoides: clinicopathological and prognostic features of 45 cases. French Study Group of Cutaneous Lymphomas. *Blood* 2000; 95: 2212–2218.
 23. Nielsen PR, Eriksen JO, Lindahl LM, Wehkamp U, Bzorek M, Andersen G, et al. Diagnostic two-gene classifier in early-stage mycosis fungoides: a retrospective multicenter study. *J Invest Dermatol* 2021; 141: 213–217.e5.
 24. Nielsen PR, Eriksen JO, Wehkamp U, Lindahl LM, Gniadecki R, Fogh H, et al. Clinical and histological characteristics of mycosis fungoides and Sézary syndrome: a retrospective, single-centre study of 43 patients from eastern Denmark. *Acta Derm Venereol* 2019; 99: 1231–1236.
 25. Olsen E, Vonderheid E, Pimpinelli N, Willemze R, Kim Y, Knobler R, et al. Revisions to the staging and classification of mycosis fungoides and Sezary syndrome: a proposal of the International Society for Cutaneous Lymphomas (ISCL) and the cutaneous lymphoma task force of the European Organization of Research and Treatment of Cancer (EORTC). *Blood* 2007; 110: 1713–1722.
 26. Bzorek M, Stamp IM, Petersen BL, Frederiksen L. Use of commercially available rabbit monoclonal antibodies for immunofluorescence double staining. *Appl Immunohistochem Mol Morphol* 2008; 16: 387–392.
 27. Benjamini Y, Krieger AM, Yekutieli D. Adaptive linear step-up procedures that control the false discovery rate. *Biometrika* 2006; 93: 491–507.
 28. Van Der Putte SCJ, Toonstra J, Van Wichen DF. B cells and plasma cells in mycosis fungoides. A study including cases with B cell follicle formation or a monotypical plasma cell component. *Am J Dermatopathol* 1989; 11: 509–516.
 29. Theurich S, Schlaak M, Steguweit H, Heukamp LC, Wennhold K, Kurschat P, et al. Targeting tumor-infiltrating B cells in cutaneous T-cell lymphoma. *J Clin Oncol* 2014; 32: 110–116.
 30. Iliadis A, Koletsis T, Patsatsi A, Georgiou E, Sotiriadis D, Kostopoulos I, et al. The cellular microenvironment and neoplastic population in mycosis fungoides skin lesions: a clinicopathological correlation. *Eur J Dermatol* 2016; 26: 566–571.
 31. Benner MF, Jansen PM, Vermeer MH, Willemze R. Prognostic factors in transformed mycosis fungoides: a retrospective analysis of 100 cases. *Blood* 2012; 119: 1643–1649.
 32. Barberio E, Thomas L, Skowron F, Balme B, Dalle S. Transformed mycosis fungoides: clinicopathological features and outcome. *Br J Dermatol* 2007; 157: 284–289.
 33. Nelson BH. CD20 + B cells: the other tumor-infiltrating lymphocytes. *J Immunol* 2010; 185: 4977–4982.
 34. Milne K, Köbel M, Kalloger SE, Barnes RO, Gao D, Gilks CB, et al. Systematic analysis of immune infiltrates in high-grade serous ovarian cancer reveals CD20, FoxP3 and TIA-1 as positive prognostic factors. *PLoS One* 2009; 4: e6412.
 35. Tadmor T, Zhang Y, Cho HM, Podack ER, Rosenblatt JD. The absence of B lymphocytes reduces the number and function of T-regulatory cells and enhances the anti-tumor response in a murine tumor model. *Cancer Immunol Immunother* 2011; 60: 609–619.
 36. Olkhanud PB, Damdinsuren B, Bodogai M, Gress RE, Sen R, Wejksza K, et al. Tumor-evoked regulatory B cells promote breast cancer metastasis by converting resting CD4+ T cells to T-regulatory cells. *Cancer Res* 2011; 71: 3505–3515.
 37. Ghosn S, Bahhady R, Mahfouz R, Abbas O, Kibbi AG, Saad R, et al. Concomitant occurrence of kimura disease and mycosis fungoides in a lebanese woman: significance and response to rituximab. *Am J Dermatopathol* 2009; 31: 814–818.
 38. Czarnowicki T, Gonzalez J, Bonifacio KM, Shemer A, Xiangyu P, Kunjrvia N, et al. Diverse activation and differentiation of multiple B-cell subsets in patients with atopic dermatitis but not in patients with psoriasis. *J Allergy Clin Immunol* 2016; 137: 118–129.
 39. Simon D, Hösli S, Kostylina G, Yawalkar N, Simon HU. Anti-CD20 (rituximab) treatment improves atopic eczema. *J Allergy Clin Immunol* 2008; 121: 122–128.
 40. Jimenez-Boj E, Stamm TA, Sadlonova M, Rovensky J, Rafayová H, Leeb B, et al. Rituximabin psoriatic arthritis: an exploratory evaluation. *Ann Rheum Dis* 2012; 71: 1868–1871.
 41. Kersh AE, Feldman RJ. Autoimmune sequelae following rituximab therapy: a review of the literature and potential immunologic mechanisms. *J Clin Rheumatol* 2018; 24: 427–435.